

# Vascular endothelial growth factor stimulates dephosphorylation of the catenins p120 and p100 in endothelial cells

Elaine Y. M. WONG, Louise MORGAN, Caroline SMALES, Paul LANG, Sharon E. GUBBY and James M. STADDON<sup>1</sup>

Eisai London Research Laboratories Ltd., Bernard Katz Building, University College London, Gower Street, London WC1E 6BT, U.K.

Vascular endothelial growth factor (VEGF) is an endothelium-specific mitogen that induces angiogenesis and increases vascular permeability. These processes involve regulation of cell–cell adhesion, but molecular mechanisms have yet to be fully established. p120, also termed p120<sup>cas</sup>, and its variant p100 are catenins which associate with cadherins and localize to adherens junctions. VEGF was reported to stimulate tyrosine phosphorylation of catenins in endothelial cells. In contrast, we have found that VEGF potently stimulated a rapid and dose-dependent decrease in serine/threonine phosphorylation of p120 and p100. VEGF acted via VEGF receptor 2 to achieve this effect which was independent of activation of the

extracellular-signal-regulated kinase pathway. Histamine and activators of protein kinase C had a very similar effect to that of VEGF on phosphorylation of p120 and p100, suggesting that these diverse stimuli may converge on a common signalling element regulating p120/p100 serine/threonine phosphorylation. These data raise the possibility that the dephosphorylation of p120 and p100 triggered by VEGF may contribute to mechanisms regulating permeability and/or motility through modulation of cadherin adhesiveness.

**Key words:** adherens junction, angiogenesis, cadherin, phosphorylation.

## INTRODUCTION

Vascular endothelial growth factor (VEGF) is an endothelial-specific mitogen, angiogenic factor and permeability enhancing factor, important in both normal development and physiology as well as in pathological situations [1,2]. In humans, a single VEGF gene gives rise to multiple splice variants, differing in secretory and heparin-binding properties [3]. Dimers of VEGF bind to the tyrosine kinase receptors VEGF receptor 1 [VEGFR-1; also known as fms-like tyrosine kinase-1 (Flt-1)] and VEGFR-2 [also known as kinase insert domain-containing receptor (KDR) and foetal liver kinase-1 (Flk-1)], resulting in receptor trans-tyrosine phosphorylation and, through SH2 domains, recruitment of down-stream signalling effectors [4]. The role of these signalling events, including activation of phosphatidylinositol 3-kinase, extracellular signal regulated kinases (ERKs), phospholipase C and focal adhesion kinase (FAK), is under investigation (see e.g. [5–10]).

VEGF also appears to stimulate the tyrosine phosphorylation of cadherin and catenins in endothelial cells [11]. Classic cadherins are homophilically interacting, calcium-dependent, single-pass transmembrane glycoproteins that form the basis of adherens junctions in endothelial and epithelial cells. For function, cadherins associate with cytoplasmic proteins termed catenins. Binding to  $\beta$ - or  $\gamma$ -catenin is direct and via the C-terminal region of cadherin, whereas  $\alpha$ -catenin, a vinculin homologue that links the complex to the actin-based cytoskeleton, binds via  $\beta$ -catenin [12–17].

p120 was originally discovered as an Src substrate, and its tyrosine phosphorylation may be involved in cellular transformation [18]. It was realised subsequently to be associated with cadherins in both epithelial and endothelial cells [19–21]. Splice variants of p120, including p100, also exist [19,21–23]. More

recently, the juxtamembrane region of cadherin has also been found to affect its adhesive properties; as this binds p120, it implies that this is a functionally significant interaction [24,25].

Previous experiments had shown that pharmacological agents such as the protein kinase C activator phorbol-12,13-dibutyrate (PDB) [26,27] and inflammatory agents such as histamine [27] could activate a pathway leading to serine/threonine dephosphorylation of p120/p100. In the present report, we present evidence that in endothelial cells VEGF does not stimulate tyrosine phosphorylation of catenins. Rather, VEGF, in a manner that is remarkably similar to that triggered by histamine and PDB, also regulates serine/threonine phosphorylation of p120 and p100.

## MATERIALS AND METHODS

### Chemicals and reagents

VEGF<sub>165</sub> was from PeproTech EC Ltd. (London, U.K.), placenta growth factor was from R & D Systems Europe Ltd. (Oxford, U.K.) and PDB was from Calbiochem–Novabiochem (Nottingham, U.K.). Histamine and V8 protease (P-6306) were from Sigma Chemical Co., SU 5416 was from Tsukuba Research Laboratories (Eisai Co., Tsukuba, Japan) and collagen (Vitrogen 100) was from Imperial Laboratories (Andover, Hants, U.K.). [<sup>32</sup>P]Phosphate (10 mCi/ml, carrier free) was from ICN-Flow Laboratories and alkaline phosphatase was from Boehringer.

### Antibodies

Mouse monoclonal antibodies recognizing VE-cadherin (cadherin-5), N-cadherin, p120 and p100,  $\beta$ -catenin, phosphotyrosine (antibody PY20), FAK, paxillin, p42 ERK and the

Abbreviations used: ERK, extracellular signal regulated kinase; FAK, focal adhesion kinase; HUVECs, human umbilical vein endothelial cells; PDB, phorbol-12,13-dibutyrate; VEGF, vascular endothelial growth factor; VEGFR, VEGF receptor; KDR, kinase insert domain-containing receptor; Flk-1, foetal liver kinase-1.

<sup>1</sup> To whom correspondence should be addressed (e-mail James\_Staddon@eisai.net).

rabbit polyclonal anti-phosphotyrosine antibody, were from Transduction Laboratories (Lexington, KY, U.S.A.). Peptide-directed antibodies recognizing  $\alpha$ - and  $\gamma$ -catenin were provided by Kurt Herrenknecht (Eisai London Research Laboratories, University College London, London, U.K.). Rabbit polyclonal antibody (catalogue no. 9101) recognizing the activated forms (phosphoThr<sup>202</sup>/phosphoTyr<sup>204</sup>) of p42 and p44 ERK (also known as mitogen-activated protein kinase) was from New England BioLabs. Mouse monoclonal anti-vinculin antibody (VIN-11-5) was from Sigma and mouse monoclonal antibodies recognizing ZO-1 and CD31 were from Zymed and Dako respectively. Horseradish peroxidase-conjugated secondary antibodies were from Amersham. Fluorochrome-conjugated (Cy3 or fluorescein) secondary antibodies and rabbit anti-mouse IgG were from Jackson ImmunoResearch Labs (West Grove, PA, U.S.A.).

### Cells and Treatments

Human umbilical vein endothelial cells (HUVECs), pooled donors, were from BioWhittaker (Wokingham, Berks., U.K.) and cultured in endothelial growth medium (EGM; BioWhittaker) on collagen-coated plastic flasks (Falcon) according to the supplier's instructions. Stocks were maintained in 75 cm<sup>2</sup> flasks and split at a 1:3 ratio when almost confluent. For experiments, cells were seeded such that confluence was established within 2–3 days and the cells were usually used 5–6 days after seeding. For experiments, the cells were equilibrated in fresh medium for at least 2 h prior to the start of the experiment. Compounds and agents that were only soluble as stocks in DMSO were added to the culture medium of the cells in an equal volume of CO<sub>2</sub>- and temperature-equilibrated medium containing twice the finally required concentration of compound. The final concentration of DMSO did not exceed 0.1% (v/v). Aqueous soluble agents were added at a 1:100 dilution directly to the cultures. In all cases, appropriate vehicle controls were performed and found to have no effect.

[<sup>32</sup>P]Phosphate labelling was performed using Puck's Saline A (P-2917; Sigma) supplemented with 10 mM HEPES (Gibco), 2 mM glutamine (Gibco), 1 mM CaCl<sub>2</sub>, 1 mM MgSO<sub>4</sub> and 0.2% (v/v) foetal calf serum. Cultures were rinsed twice with this medium and then incubated with medium containing 100  $\mu$ Ci/ml of [<sup>32</sup>P]phosphate. Labelling was for 2 h at 37 °C in humidified air with ambient CO<sub>2</sub>.

### Protein analysis

Methods have been described previously for: preparation of cell lysates, SDS/PAGE and immunoblotting [27]; immunoprecipitation analysis of cadherin and its association with catenins using Triton X-100 lysis buffer (TXLB) [27]; p120/p100-specific and phosphotyrosine protein immunoprecipitations using SDS sample buffer (SDSSB) lysis buffer [28].

For phosphorylation analysis, cells were labelled with [<sup>32</sup>P]orthophosphate. After treatments, cells were lysed in boiling SDSSB and immunoprecipitated with the anti-p120/p100 antibody as described in [28]. After separation by SDS/PAGE, for quantification of [<sup>32</sup>P]phosphate incorporation into p120/p100, protein was transferred to nitrocellulose and [<sup>32</sup>P]phosphate was detected by autoradiography. The filter was then probed with antibody recognizing p120 and p100 to quantify protein levels. For both, preflashed film was used. Phosphoamino acid analysis procedures have been described ([29] and see [27]). Proteolytic maps [30] were obtained from immunoprecipitated protein

resolved by SDS/PAGE and detected by autoradiography. Slices of gel containing p120 and p100 were excised, rehydrated in TSE buffer [0.5 M Tris/HCl, pH 6.8, 0.1% SDS, 1 mM EDTA (tetrasodium salt)] containing 20% (v/v) glycerol, inserted into the well of the stacking gel containing 1 mM EDTA (tetrasodium salt) and overlaid with TSE buffer containing 10% glycerol and 100 ng of V8 protease. Following electrophoresis, the 15% (w/v) polyacrylamide gel (again containing EDTA) was fixed, dried and autoradiographed at –80 °C.

Phosphatase treatment *in vitro* was performed on p120/p100-specific immunoprecipitations. Following the final wash of the beads, they were then washed a further two times in phosphatase buffer comprising 50 mM Tris/HCl, pH 8.8, 0.1 M NaCl, 1 mM MgCl<sub>2</sub> and 1% (v/v) Triton X-100. The beads were then incubated with 100  $\mu$ l of phosphatase buffer containing protease inhibitors (as for immunoprecipitation procedures), supplemented with or without alkaline phosphatase (50 units) in the absence or presence of a cocktail of phosphatase inhibitors (4 mM EDTA, 25 mM NaF, 50 mM  $\beta$ -glycerophosphate and 1 mM Na<sub>3</sub>VO<sub>4</sub>). After incubation at 30 °C for 1 h, reactions were then quenched by the addition of 1 ml of phosphatase buffer containing the phosphatase inhibitors. The beads were removed by centrifugation, the supernatant was removed and the protein eluted into sample buffer. p120 and p100 were then analysed by SDS/PAGE and immunoblotting.

### Immunocytochemistry

Confluent cultures of cells on 0.4  $\mu$ m pore size, collagen-coated polycarbonate Transwell filters (Costar) were used for immunolabelling. After treatments, the cells were fixed at room temperature for 10 min in 4% (w/v) paraformaldehyde made up in PBS. Fixed cells were rinsed and then permeabilized by incubation in 0.5% Triton X-100 in PBS for 30 min. For labelling, all antibodies were diluted in PBS with 10% (v/v) foetal calf serum, 100 mM lysine, 0.3% Triton X-100 and 0.02% sodium azide. Labelling with protein-specific antibodies was performed overnight at 4 °C, and that with the rabbit anti-phosphotyrosine antibody was for 2 h at room temperature. Secondary antibodies recognizing mouse or rabbit IgG conjugated to fluorescein or Cy3 respectively, were applied together for 1 h at room temperature. After rinsing, the samples were mounted under Citifluor and viewed using a Leica TCS SP confocal microscope. The stage was advanced in steps of 10 nm until optimal images of protein-specific staining were achieved. The two fluorophores were sequentially scanned and overlaid giving a composite two-channel view of a single optical plane.

## RESULTS

### VEGF stimulates an increase in p120/p100 electrophoretic mobility

Monolayers of HUVECs were incubated in the absence or presence of 2.6 nM (100 ng/ml) VEGF<sub>165</sub> for 5 min. Following extraction of the cells into Laemmli sample buffer, resolution of cell protein by SDS/PAGE and electrotransfer to nitrocellulose, the immunoblots (Figure 1A) revealed p120 and p100 migrating as broad bands when extracted from control cells. After incubation of the cells with VEGF, p120 and p100 migrated as faster, tighter bands. The different lanes in Figure 1(A) are derived from extracts of separate cultures in the experiment. This observation was made with cells at very early passage (P2) and could be consistently observed even up to passage 10.

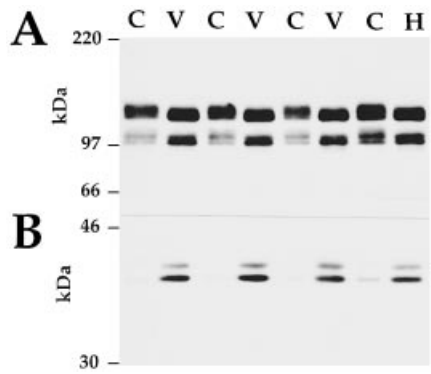


**Figure 1 VEGF stimulates a p120/p100 mobility shift in endothelial cells**

Confluent monolayers of HUVECs were incubated in the absence (C) or presence of 2.6 nM (100 ng/ml) VEGF (V) for 5 min. In parallel, some cells were treated for 5 min with 10  $\mu$ M histamine (H). (A) Cell extracts were prepared and p120 (○) and p100 (●) were detected by immunoblotting following SDS/PAGE. (B) The same filter was also probed with an antibody recognizing the activated forms of p42 and p44 ERKs (arrowheads). All lanes received equal amounts of protein as determined by Ponceau S staining of the filters and verification by reprobing with antibody recognizing  $\beta$ -catenin (results not shown).

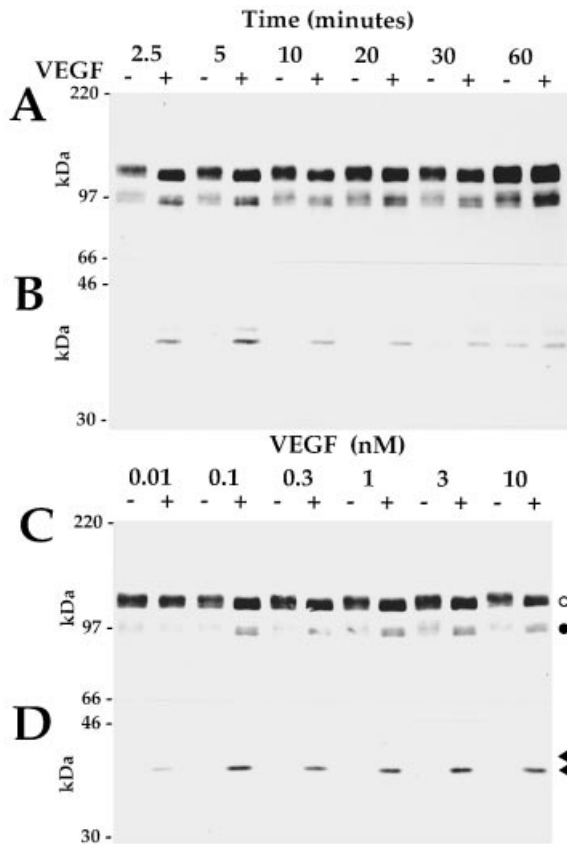


**Figure 2 VEGF acts rapidly and potently**

Confluent monolayers of HUVECs were incubated in the absence (–) or presence (+) of 2.6 nM (100 ng/ml) VEGF for the times indicated. (A) Cell extracts were prepared and p120 (○) and p100 (●) were detected by immunoblotting following SDS/PAGE. (B) The filter from (A) was also probed with the antibody recognizing the activated forms of p42 and p44 ERKs (arrowheads). In a separate experiment, confluent monolayers of HUVECs were incubated for 5 min in the absence (–) or presence (+) of the indicated concentrations of VEGF. (C) Cell extracts were prepared and p120 (○) and p100 (●) were detected by immunoblotting following SDS/PAGE. (D) The filter from (C) was also probed with the antibody recognizing the activated forms of p42 and p44 ERKs (arrowheads). For both experiments, equal loading of lanes was verified as in Figure 1.

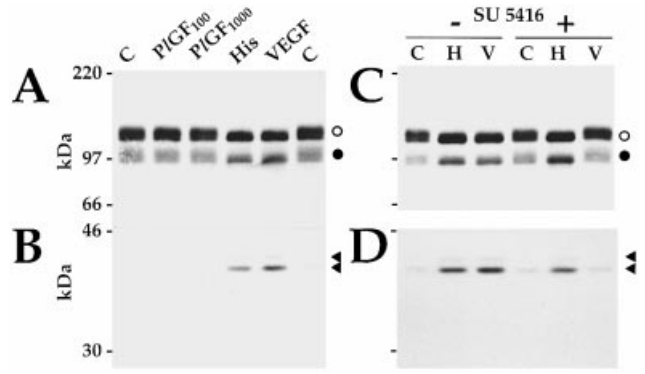


**Figure 3 VEGF acts via VEGFR-2 (KDR/Fik-1)**

(A and B) Confluent monolayers of HUVECs were incubated for 5 min in the absence (C) or presence of placenta growth factor at 100 (P/GF<sub>100</sub>) or 1000 ng/ml (P/GF<sub>1000</sub>). In parallel, cells were treated with either 10  $\mu$ M histamine (His) or 2.6 nM (100 ng/ml) VEGF. (C and D) Cells were preincubated for 30 min in the absence (–) or presence (+) of the VEGFR-2 inhibitor SU 5416 (5  $\mu$ M). The cells were then treated for 5 min with either 2.6 nM VEGF (V) or 10  $\mu$ M histamine (H). (A and C) In all cases, cell extracts were prepared and p120 (○) and p100 (●) were detected by immunoblotting following SDS/PAGE. (B and D) The filters from (A) and (C) respectively were also probed with antibody recognizing the activated forms of p42 and p44 ERKs (arrowheads). Equal loading of lanes was verified as in Figure 1.

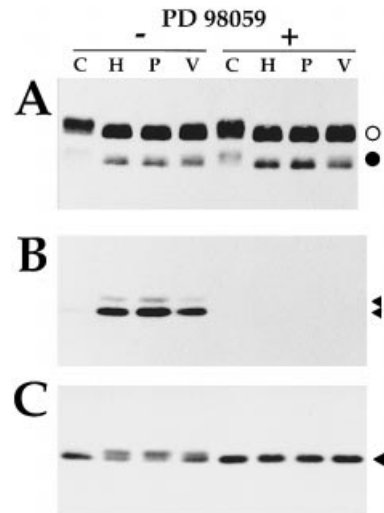


**Figure 4 The role of the ERK pathway**

Confluent monolayers of HUVECs were preincubated for 30 min with or without 50  $\mu$ M of the ERK kinase inhibitor PD 98059. The cells were then treated with vehicle (C), 10  $\mu$ M histamine (H), 200 nM PDB (P) or 2.6 nM VEGF (V) for 5 min. Cell extracts were prepared and following SDS/PAGE, immunoblotting was performed to detect: (A) p120 (○) and p100 (●), (B) activated forms of p42 and p44 ERKs (arrowheads), and (C) a reprobe of (B) with p42 ERK (arrowhead).

For comparative purposes, the cells were also incubated for 5 min with 10  $\mu$ M histamine. Histamine also stimulated an increase in electrophoretic mobility of p120 and p100, as reported previously [27], and this was very similar to that elicited by VEGF (Figure 1A). To reveal other changes in VEGF-stimulated signalling processes, the filters were also probed with an antibody recognizing the activated forms of p42 and p44 ERK. VEGF and histamine clearly stimulated an increase in phosphorylation of

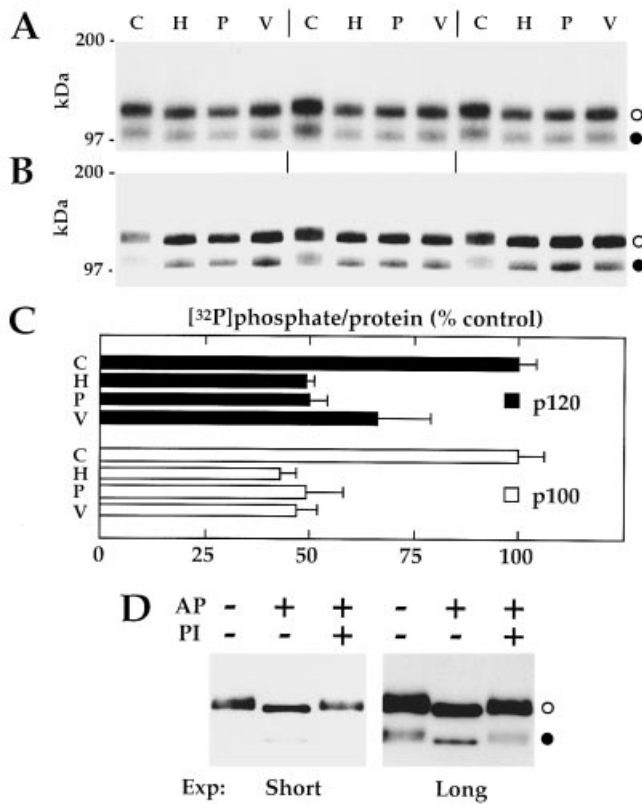


**Figure 5** VEGF induces dephosphorylation of p120 and p100

Confluent monolayers of HUVECs were metabolically labelled with [ $^{32}$ P]phosphate. The cells were then treated for 5 min with vehicle (C), 10  $\mu$ M histamine (H), 200 nM PDB (P) or 2.6 nM VEGF (V). Following lysis in TDS buffer, p120 and p100 were immunoprecipitated, resolved by SDS/PAGE and transferred to nitrocellulose. (A) An autoradiogram of the filter was taken to detect [ $^{32}$ P]phosphate incorporation into p120 (○) and p100 (●), and the filter was then probed with antibody recognizing p120 and p100 to detect protein (B). Autoradiography was for 40 h at  $-80^{\circ}\text{C}$  and the ECL\* exposure was taken in 1 min. Band densities in the autoradiogram and luminogram were quantified by densitometry and the [ $^{32}$ P]phosphate incorporation normalized to protein is expressed in (C). (D) The effects of *in vitro* dephosphorylation on the electrophoretic mobility of p120 (○) and p100 (●). HUVEC cultures were lysed and p120/p100 specifically immunoprecipitated as described in the Materials and methods section. The immunoprecipitates were washed twice in phosphatase buffer and then incubated in the absence (–) or presence (+) of alkaline phosphatase (AP) and a cocktail of phosphatase inhibitors (PI). The short exposure (Exp:) shows p120 (○) migrating as a broad band which becomes compressed and more intense following phosphatase treatment. Similarly, the longer exposure clearly shows p100 (●) migrating as a broad band of low intensity which becomes a tighter, darker band after phosphatase treatment. The action of the preparation of phosphatase was blocked by the cocktail of phosphatase inhibitors.

the ERKs in parallel with their ability to affect p120/p100 migration (Figure 1B).

### VEGF acts quickly and potently

VEGF acted very rapidly to trigger the increase in mobility of p120 and p100. Effects were observed within 2 min and sustained for up to 30 min (Figure 2A). After 60 min of incubation, the effect was less apparent. The kinetics paralleled those of the increase in ERK phosphorylation (Figure 2B). VEGF was also very potent at affecting p120/p100 mobility; effects were observed with concentrations as low as 0.1 nM (Figure 2C). The sensitivity of the increase in ERK phosphorylation paralleled that of the increase in p120/p100 mobility (Figure 2D).

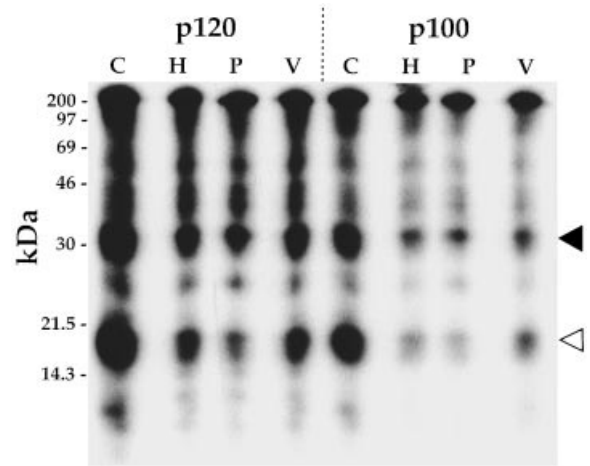


**Figure 6** VEGF induces dephosphorylation of both p120 and p100 at similar sites

Confluent monolayers of HUVECs were metabolically labelled with [ $^{32}$ P]phosphate. The cells were then treated for 5 min with vehicle (C), 10  $\mu$ M histamine (H), 200 nM PDB (P) or 2.6 nM VEGF (V). Following lysis in TDS buffer, p120 and p100 were immunoprecipitated and resolved by SDS/PAGE. The gel was briefly fixed and an autoradiogram taken to localize bands corresponding to p120 and p100. These were excised from the gel, partially digested with V8 protease and the digestion products were analysed by SDS/PAGE. The labelling of digestion products was detected again by autoradiography. It was confirmed by immunoblotting that the amounts of p120 and p100 in the initial immunoprecipitates were equal. Two major partial digestion products from both p120 and p100 were detected at 30 kDa and 17 kDa (arrowheads). Treatment with VEGF, histamine or PDB resulted in a decrease in labelling of both of these two products, suggesting that all three agents affected phosphorylation of p120 and p100 at similar sites.

### VEGF acts through VEGFR-2

VEGF is known to bind to two receptors, VEGFR-1 and VEGFR-2. Placenta growth factor, a VEGFR-1-specific ligand, even at concentrations up to 1000 ng/ml, failed to stimulate either a mobility shift in p120/p100 (Figure 3A) or ERK phosphorylation (Figure 3B), whereas appropriate positive controls were effective. These observations suggest by default that VEGF acted via VEGFR-2. This was corroborated by demonstrating that the VEGFR-2-specific inhibitor SU 5416 [31] blocked the ability of VEGF to stimulate an increase in p120/p100 mobility (Figure 3C) and ERK phosphorylation (Figure 3D). In contrast, SU 5416 had no effect on the actions of histamine (Figures 3C and 3D), indicating selectivity in its mode of action.

### VEGF action on p120 does not require activation of the ERK pathway

PD 98059, a pharmacological inhibitor of ERK kinase activation [32], did not block the ability of VEGF, histamine and PDB to trigger a mobility shift in p120 and p100 (Figure 4A). Demonstrating the efficacy of the inhibitor was the complete suppression of the increases in ERK phosphorylation [revealed either by the phospho-epitope antibody (Figure 4B) or by the band-shift in p42 ERK (Figure 4C)] without affecting, as a control, p42 ERK expression and detection (Figure 4C). Therefore, it appears that the activation of the ERK pathway, at least at the level of ERK and ERK kinase, is not connected to pathways affecting p120.

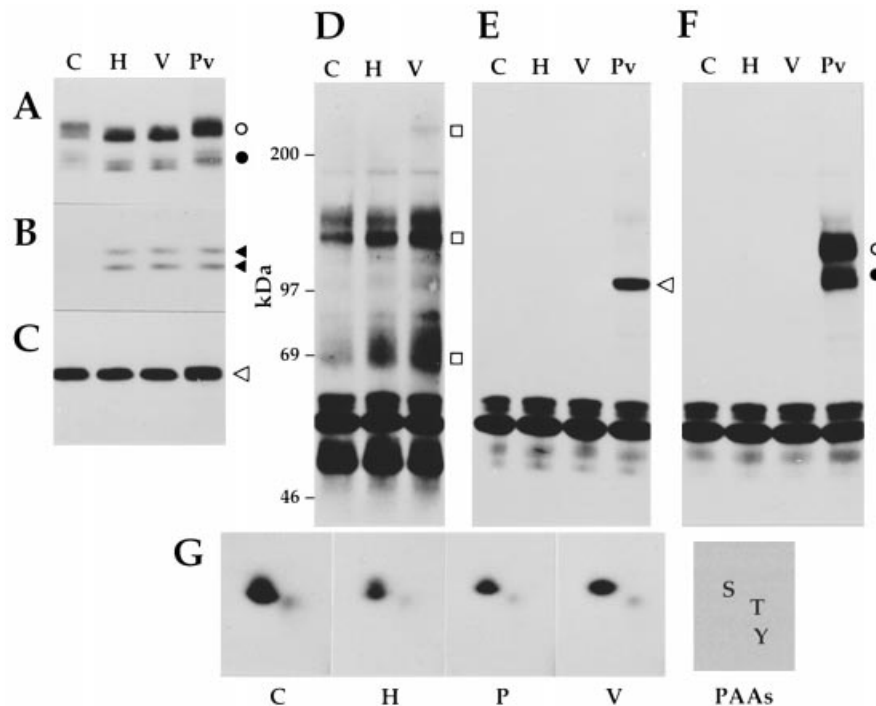


**Figure 7** VEGF stimulates serine/threonine dephosphorylation of p120 and p100 and does not affect tyrosine phosphorylation

Confluent monolayers of HUVECs were treated for 5 min in the absence (C) or presence of either 10  $\mu$ M histamine (H) or 2.6 nM VEGF (V). Some cells were treated for 15 min with 100  $\mu$ M pervanadate (Pv). All cultures were lysed in boiling buffer containing SDS, as described in the Materials and methods section. Aliquots of the extract were analysed by SDS/PAGE for (A) p120 (○) and p100 (●), (B) the activated forms of p42 and p44 ERKs (arrowheads), and (C)  $\beta$ -catenin. (D) The extracts were then immunoprecipitated using the anti-phosphotyrosine antibody PY20 and analysed by immunoblotting with PY20. In this case, the pervanadate treatment resulted in a signal that was too strong to be shown relative to that obtained with the other treatments (result not shown). The open squares indicate the migration of bands that, on the basis of their apparent molecular mass correspond, in order of decreasing size, to VEGFR-2, FAK and paxillin. The tentative identification of paxillin and FAK was confirmed by reprobing the filters with protein-specific antibodies (results not shown but see [6]). The PY20 immunoprecipitates were also probed with antibody recognizing (E)  $\beta$ -catenin (open arrow head) and (F) p120 (○) and p100 (●). (G) Phosphoamino acid analysis. Confluent monolayers of HUVECs were metabolically labelled with [ $^{32}$ P]phosphate and received either vehicle (C), 10  $\mu$ M histamine (H), 200 nM PDB (P) or 2.6 nM VEGF (V) for 5 min. Following lysis in TDS buffer and immunoprecipitation, phosphoamino acid analysis of p120 and p100 was performed as described in the Materials and methods section. The migration of phosphoamino acid standards (PAAs) is also shown. S, phosphoserine; T, phosphothreonine; Y, phosphotyrosine.

### VEGF stimulates p120/p100 dephosphorylation

The basis of the increase in mobility of p120/p100 stimulated by VEGF was further analysed by metabolically labelling cells with [ $^{32}$ P]phosphate. Lysis of cells was in harshly denaturing buffer designed to preserve the phosphorylation state of proteins. Autoradiography and immunoblotting of immunoprecipitates allows determination of phosphate/protein ratios. The [ $^{32}$ P]-phosphate/protein ratio of p120 and p100 in control cells was estimated by this method (Figures 5A–5C). After VEGF stimulation, the autoradiogram showed that the [ $^{32}$ P]phosphate signal was less and the film density was similar to that of p120/p100 from control cells (Figure 5A). The corresponding immunoblot (Figure 5B) showed that VEGF caused an increase in p120/p100 mobility and an increase in film density of the signal. Densitometry quantified the VEGF-stimulated dephosphorylation of p120 and p100 (Figure 5C), and this dephosphorylation was similar in magnitude to that elicited by histamine or PDB (Figures 5A–5C). In response to VEGF, histamine and PDB, p120/p100 are dephosphorylated resulting in increased electrophoretic mobility. The autoradiogram shows less of a signal whereas the immunoblot shows an increased intensity as protein is concentrated on to a smaller area of the filter. In all cases, the supernatants from the immunoprecipitations were analysed by SDS/PAGE and autoradio-

graphy to confirm that there were no general effects on the phosphorylation of the many proteins present in these fractions (results not shown).

The phosphorylation-dependent electrophoretic mobility of p120/p100 was also explored by *in vitro* dephosphorylation. Immunoprecipitation of p120/p100 followed by incubation in phosphatase buffer alone still allowed detection of p120 and p100 as broad bands (Figure 5D), although, for reasons that are not completely clear, the amount of p100 seemed to be less when compared with the usual immunoprecipitations (Figure 5A). Nevertheless, phosphatase treatment altered the electrophoretic mobility of p120/p100 with the result that the bands became tighter and more intense. The activity of the phosphatase preparation was indeed attributable to dephosphorylation, as indicated by the prevention of this effect by phosphatase inhibitors (Figure 5D). Thus, *in vitro* dephosphorylation produces effects on the electrophoretic mobility of p120/p100 that are similar to those produced by treatment of intact cells with VEGF, histamine and PDB.

### Discrete sites of phosphorylation

The pattern of phosphorylation sites within p120/p100 was analysed. Following labelling with [ $^{32}$ P]phosphate and stimu-



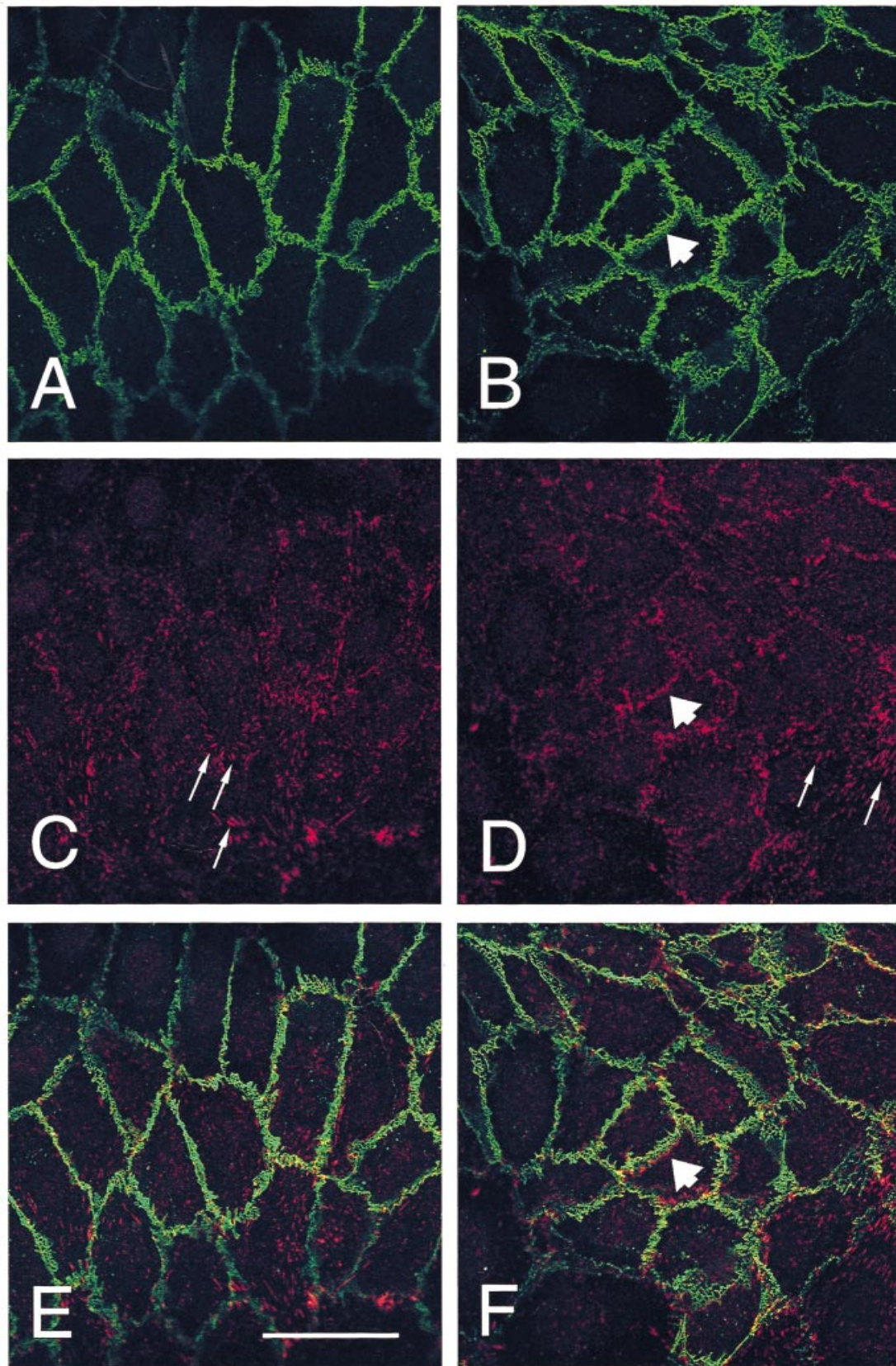


**Figure 8** VEGF stimulation does not increase protein phosphotyrosine of adherens junction-associated proteins

HUVECs were either treated with vehicle (**A**, **C** and **E**) or 2.6 nM VEGF (**B**, **D** and **F**). After 5 min the cells were fixed, permeabilized and then co-labelled with mouse antibody recognizing p120/p100 (**A** and **B**) and rabbit anti-phosphotyrosine (**C** and **D**). The confocal microscope was used to focus optimally on the p120/p100 labelling and the corresponding phosphotyrosine labelling pattern

lation as required, Cleveland mapping, a procedure involving limited proteolytic digestion, was performed. It was confirmed by immunoblotting that equal amounts of protein were analysed for each condition. For both p120 and p100, two major cleavage products at 30 kDa and 17 kDa were observed when protein was extracted from control cells (Figure 6). After VEGF stimulation, phosphate incorporation into both of these fragments was substantially decreased (Figure 6), and similar effects of histamine and PDB were noted (Figure 6), suggesting that these different stimuli affect p120 and p100 phosphorylation at similar sites.

### Amino acid residues affected

HUVECs were incubated with histamine, VEGF or the broad-spectrum tyrosine phosphatase inhibitor pervanadate (see [28]). To prevent any post-lysis artefacts, lysates of the cells were prepared by immediate extraction into a boiling solution of an SDS-based buffer containing kinase and phosphatase inhibitors. As positive controls, these extracts were analysed to show that VEGF and histamine produced effects on p120/p100 mobility (Figure 7A) and ERK phosphorylation (Figure 7B). Pervanadate did not affect the mobility of p120/p100 (Figure 7A) but did lead to ERK phosphorylation (Figure 7B). The levels of  $\beta$ -catenin were found to be similar in all extracts (Figure 7C).

The extracts were then immunoprecipitated and immunoblotted with anti-phosphotyrosine antibody PY20 (Figure 7D). In the controls, several major bands were observed. As perhaps expected [33], histamine stimulated an increase in tyrosine phosphorylation of bands identified (see legend to Figure 7) as paxillin (approx. 69 kDa) and FAK (125 kDa). VEGF had similar effects and, additionally, produced effects on tyrosine phosphorylation of a band with an apparent molecular mass consistent with that of the VEGFR-2, again as expected [6]. Therefore, the protein tyrosine phosphorylation pattern of the cells used in the present study was very similar to that reported by other laboratories.

The same PY20 immunoprecipitates were then probed with antibodies recognizing  $\beta$ -catenin (Figure 7E) or p120/p100 (Figure 7F). Only after treatment with pervanadate were  $\beta$ -catenin and p120/p100 detected in the phosphotyrosine immunoprecipitates. A ten-times overexposure of the filters did not reveal any hint of  $\beta$ -catenin or p120/p100 in the phosphotyrosine immunoprecipitates in response to VEGF or histamine (results not shown). Therefore, even though the PY20 immunoprecipitates revealed tyrosine phosphorylation of proteins already reported to be tyrosine phosphorylated in response to VEGF and histamine, these same immunoprecipitates did not contain  $\beta$ -catenin or p120/p100.

Phosphoamino acid analysis of p120/p100 was also performed. In control cells, p120 and p100 were phosphorylated on mainly serine and, to a lesser extent, threonine residues (Figure 7G). No phosphotyrosine was detected. After stimulation with VEGF, phosphotyrosine was not detected but the amounts of phosphoserine and phosphothreonine were decreased. Similar results were obtained after histamine and PDB treatment (Figure 7G; previous experiments [27] were done with EA.hy926 cells). These observations indicate that p120 and p100 were dephosphorylated on serine and threonine residues in response to the various treatments.

### Immunocytochemical analysis of phosphorylation

Possible effects on protein tyrosine phosphorylation of catenins were also examined immunocytochemically. In control cells, p120/p100 were detected at cell-cell contacts in a fine, continuous pattern (Figure 8A). VEGF treatment had no effect on this pattern (Figure 8B). The labelling pattern of  $\beta$ -catenin was similarly unaffected (results not shown). In control cells, the corresponding labelling of tyrosine phosphorylated protein revealed mainly striations (Figure 8C, arrows) that co-labelled with anti-vinculin, paxillin or FAK antibodies (results not shown), identifying them as focal contacts. The merged image (Figure 8E) shows very occasional overlap of the two fluorophores. At the focal plane of p120/p100, the phosphotyrosine labelling was altered in a subtle way after VEGF treatment. This was revealed as the development of an almost continuous pattern that is seen in some but not all cells in this particular image (Figure 8D, large arrow). In several other experiments, similar effects were observed. This labelling pattern, although adjacent to, did not co-localize with that of p120/p100 (Figure 8F, arrow), nor for that matter with that of ZO-1 or CD31 (results not shown). As reported by others [6], VEGF did stimulate focal contact formation (images not shown) but this is not seen clearly in the confocal images presented here which show single optical sections focusing on co-localization with catenins.

### Stoichiometry of the cadherin/catenin complex

Cadherins associate via their cytoplasmic tail with the catenins, including p120 and p100. To test if VEGF treatment resulted in altered association of catenins with cadherins in endothelial cells, the cells were lysed under detergent conditions designed to preserve association of the complex. Lysates from control or VEGF-stimulated (2.6 nM, 5 min) cells were immunoprecipitated with antibodies recognizing both p120 and p100 or  $\beta$ -catenin. The immunoprecipitates were analysed by immunoblotting for the content of VE-cadherin, N-cadherin,  $\alpha$ -,  $\beta$ - and  $\gamma$ -catenin, p120 and p100. VEGF treatment, although increasing the electrophoretic mobility of p120 and p100, had no effect on association of any members of the complex (results not shown). Furthermore, immunocytochemical analysis did not reveal any apparent effects on localization of p120/p100 (Figure 8) or  $\beta$ -catenin (result not shown) to adherens junctions following VEGF treatment.

### DISCUSSION

Here, we present evidence that VEGF, like histamine (see [27]) and PDB (see [26]), triggers the serine/threonine dephosphorylation of the catenins p120 and p100 in endothelial cells through activation of the VEGFR-2 and independently of activation of p42 and p44 ERKs. The Cleveland maps suggest that these diverse agents converge on a common regulatory element involved in p120 serine/threonine phosphorylation.

was then determined. (E and F) Merged images of (A and C) and (B and D) respectively. In parallel, some cells were also extracted and analysed for p120/p100 by immunoblotting to confirm that VEGF had in fact stimulated a p120/p100 shift in this experiment (results not shown). Also, it was confirmed that the phosphotyrosine labelling was blocked by labelling in the presence of phosphotyrosine but not phosphoserine or phosphothreonine. The fine arrows in (C) and (D) show distinctive striations that co-labelled with anti-vinculin antibody (results not shown), therefore identifying them as focal contacts. The larger arrows in (B, D and F) indicate a pattern where a subtle change in phosphotyrosine was produced in response to VEGF stimulation. This new pattern, although adjacent to that of p120 labelling did not co-localize with p120/p100 [see (F)], nor for that matter with vinculin (results not shown). Similar subtle changes in phosphotyrosine staining in response to VEGF were observed in several other experiments. VEGF also produced a stimulation of focal contact formation but the confocal images shown here are not optimal to show this effect. Bar, 50  $\mu$ m.

In contrast, Esser et al. [11] claim that VEGF stimulates tyrosine phosphorylation of cadherin and catenins in endothelial cells. A major difference between the experiments of Esser et al. [11] and those described here is the preincubation of their cells with vanadate, a broad-spectrum inhibitor of tyrosine phosphatases. However, Esser et al. [11] did observe effects of VEGF on protein tyrosine phosphorylation even in the presence of vanadate. It is instructive to compare the effects they observe with those of Abedi and Zachary [6] and the data reported here. The tyrosine phosphorylation patterns produced by VEGF in HUVECs as reported by Abedi and Zachary [6] were quite discrete, involving proteins like paxillin and FAK, and similar observations are reported here. In contrast, Esser et al. [11] reported much stronger stimulation of tyrosine phosphorylation of many proteins by VEGF in the presence of vanadate. The VEGF-induced activation of tyrosine kinases in the presence of vanadate presumably may result in the spurious, non-physiological tyrosine phosphorylation of proteins. Indeed, members of the Src family of tyrosine kinases are localized to adherens junctions [34], and, if these were activated by VEGF, they could have effects on catenin phosphorylation in the presence of phosphatase inhibitors.

Evidence that the juxtamembrane, p120-binding region of cadherins has functional importance in terms of regulation of cadherin function is accruing (see [24,25,35–38]). The role of p120 serine/threonine phosphorylation is not yet clear. Two recent reports, using different cell systems, present evidence for gain and loss of function of cadherin associated with serine/threonine phosphorylation of p120 [39,40]. Since agents such as VEGF and histamine are known to result in alterations in endothelial permeability and both agents regulate serine/threonine phosphorylation of p120/p100, we speculate that p120 serine/threonine phosphorylation may regulate cadherin adhesiveness and thereby tight junction permeability. However, further work, such as identification of p120 serine/threonine kinases and phosphatases, will be needed to test this hypothesis.

We would like to thank Dr Kurt Herrenknecht for antibodies recognizing  $\alpha$ - and  $\gamma$ -catenin. We would also like to thank Jonathan Ham and Catherine Bardelle for critical comments on the manuscript and Kaye Ferguson for editorial assistance. Confocal microscopy and digital imaging were done with the expert assistance of Darran Clements and Jane Pendjiky of the Biomedical Imaging Research Unit at University College London.

## REFERENCES

- Risau, W. (1997) *Nature (London)* **386**, 671–674
- Neufeld, G., Cohen, T., Gengrinovitch, S. and Poltorak, Z. (1999) *FASEB J.* **13**, 9–22
- Neufeld, G., Cohen, T., Gitay-Goren, H., Poltorak, Z., Tessier, S., Sharon, R., Gengrinovitch, S. and Levi, B. Z. (1996) *Cancer Metastasis Rev.* **15**, 153–158
- Shibuya, M., Ito, N. and Claesson-Welsh, L. (1999) *Curr. Top. Microbiol. Immunol.* **237**, 59–83
- Xia, P., Aiello, L. P., Ishii, H., Jiang, Z. Y., Park, D. J., Robinson, G. S., Takagi, H., Newsome, W. P., Jirousek, M. R. and King, G. L. (1996) *J. Clin. Invest.* **98**, 2018–2026
- Abedi, H. and Zachary, I. (1997) *J. Biol. Chem.* **272**, 15442–15451
- Kroll, J. and Waltenberger, J. (1997) *J. Biol. Chem.* **272**, 32521–32527
- Takahashi, T. and Shibuya, M. (1997) *Oncogene* **14**, 2079–2089
- Wheeler-Jones, C., Abu-Ghazaleh, R., Cospedal, R., Houliston, R. A., Martin, J. and Zachary, I. (1997) *FEBS Lett.* **420**, 28–32
- Gerber, H. P., McMurtry, A., Kowalski, J., Yan, M., Keyt, B. A., Dixit, V. and Ferrara, N. (1998) *J. Biol. Chem.* **273**, 30336–30343
- Esser, S., Lampugnani, M. G., Corada, M., Dejana, E. and Risau, W. (1998) *J. Cell Sci.* **111**, 1853–1865
- Aberle, H., Butz, S., Stappert, J., Weissig, H., Kemler, R. and Hoschuetzky, H. (1994) *J. Cell Sci.* **107**, 3655–3663
- Hulskens, J., Birchmeier, W. and Behrens, J. (1994) *J. Cell Biol.* **127**, 2061–2069
- Jou, T. S., Stewart, D. B., Stappert, J., Nelson, W. J. and Marris, J. A. (1995) *Proc. Natl. Acad. Sci. U.S.A.* **92**, 5067–5071
- Rimm, D. L., Koslov, E. R., Kebriaei, P., Cianci, C. D. and Morrow, J. S. (1995) *Proc. Natl. Acad. Sci. U.S.A.* **92**, 8813–8817
- Aberle, H., Schwartz, H. and Kemler, R. (1996) *J. Cell. Biochem.* **61**, 514–523
- Yap, A. S., Brieher, W. M. and Gumbiner, B. M. (1997) *Annu. Rev. Cell Dev. Biol.* **13**, 119–146
- Daniel, J. M. and Reynolds, A. B. (1997) *Bioessays* **19**, 883–891
- Reynolds, A. B., Daniel, J., McCrea, P. D., Wheelock, M. J., Wu, J. and Zhang, Z. (1994) *Mol. Cell. Biol.* **14**, 8333–8342
- Shibamoto, S., Hayakawa, M., Takeuchi, K., Hori, T., Miyazawa, K., Kitamura, N., Johnson, K. R., Wheelock, M. J., Matsuyoshi, N., Takeichi, M. and Ito, F. (1995) *J. Cell Biol.* **128**, 949–957
- Staddon, J. M., Smales, C., Schulze, C., Esch, F. S. and Rubin, L. L. (1995) *J. Cell Biol.* **130**, 369–381
- Mo, Y. Y. and Reynolds, A. B. (1996) *Cancer Res.* **56**, 2633–2640
- Keirsebick, A., Bonne, S., Staes, K., van Hengel, J., Nollet, F., Reynolds, A. and van Roy, F. (1998) *Genomics* **50**, 129–146
- Ozawa, M. and Kemler, R. (1998) *J. Cell Biol.* **142**, 1605–1613
- Yap, A. S., Niessen, C. M. and Gumbiner, B. M. (1998) *J. Cell Biol.* **141**, 779–789
- Ratcliffe, M. J., Rubin, L. L. and Staddon, J. M. (1997) *J. Biol. Chem.* **272**, 31894–31901
- Ratcliffe, M. J., Smales, C. and Staddon, J. M. (1999) *Biochem. J.* **338**, 471–478
- Staddon, J. M., Herrenknecht, K., Smales, C. and Rubin, L. L. (1995) *J. Cell Sci.* **108**, 609–619
- Boyle, W. J., van der Geer, P. and Hunter, T. (1991) *Methods Enzymol.* **201**, 110–149
- Cleveland, D. W., Fischer, S. G., Kirschner, M. W. and Laemmli, U. K. (1977) *J. Biol. Chem.* **252**, 1102–1106
- Fong, T. A., Shawver, L. K., Sun, L., Tang, C., App, H., Powell, T. J., Kim, Y. H., Schreck, R., Wang, X. and Risau, W. (1999) *Cancer Res.* **59**, 99–106
- Alessi, D. R., Cuenada, A., Cohen, P., Dudley, D. T. and Saltiel, A. R. (1995) *J. Biol. Chem.* **270**, 27489–27494
- Yuan, Y., Meng, F. Y., Huang, Q., Hawker, J. and Wu, H. M. (1998) *Am. J. Physiol.* **275**, H84–H93
- Tsukita, S., Oishi, K., Akiyama, T., Yamanashi, Y. and Yamamoto, T. (1991) *J. Cell Biol.* **113**, 867–879
- Kintner, C. (1992) *Cell* **69**, 225–236
- Navarro, P., Caveda, L., Breviaro, F., Mandoteanu, I., Lampugnani, M. G. and Dejana, E. (1995) *J. Biol. Chem.* **270**, 30965–30972
- Riehl, R., Johnson, K., Bradley, R., Grunwald, G. B., Cornel, E., Liliensbaum, A. and Holt, C. E. (1996) *Neuron* **17**, 837–848
- Chen, H., Paradies, N. E., Fedor-Chaikin, M. and Brackenbury, R. (1997) *J. Cell Sci.* **110**, 345–356
- Ohkubo, T. and Ozawa, M. (1999) *J. Biol. Chem.* **274**, 21409–21415
- Aono, S., Nakagawa, S., Reynolds, A. B. and Takeichi, M. (1999) *J. Cell Biol.* **145**, 551–562

Received 22 June 1999/28 October 1999; accepted 2 December 1999